

Molecular Structures and Infrared Spectra of *p*-Chlorophenol and *p*-Bromophenol. Theoretical and Experimental Studies

Wiktor Zierkiewicz,[†] Danuta Michalska,^{*,†} and Thérèse Zeegers-Huyskens[‡]

Institute of Inorganic Chemistry, Technical University of Wrocław, Wybrzeże Wyspiańskiego 27, 50-370 Wrocław, Poland, and Department of Chemistry, University of Leuven, 200F Celestijnenlaan, B3001, Heverlee, Belgium

Received: June 8, 2000; In Final Form: September 11, 2000

The molecular structures of *p*-chlorophenol and *p*-bromophenol have been calculated with the MP2, DFT-(hybrid), and HF methods using the extended 6-311++G(df, pd) basis set. The geometrical parameters of *p*-ClPh and *p*-BrPh in the gas phase have not been reported as yet. The results show that substitution of phenol with σ -electron-withdrawing groups (Br and Cl) leads to small shortening of the C–C and C–O bonds and small changes in the CCC angles. The structural changes of the phenol ring are governed mainly by the electronegativity of the para-substituent and, to a lesser extent, by resonance factors. The FT-IR spectra of *p*-ClPh, *p*-BrPh, and their OD counterparts were measured in CCl₄ and cyclohexane solutions in the frequency range of 3700–400 cm⁻¹, and the integrated infrared intensities were determined. The theoretical harmonic frequencies and infrared intensities were calculated for all the molecules using the DFT and HF methods. The best overall agreement between the calculated and experimental spectra has been obtained at the B3LYP/6-311++G(df,pd) level. A clear-cut vibrational assignment is made on the basis of the calculated potential energy distribution (PED). The effect of the *p*-Cl and *p*-Br substituents upon the characteristic phenolic frequencies and infrared intensities is discussed; in particular, it is shown that both the OH and OD torsional frequencies are related to the nature of the substituent.

Introduction

Phenol has been the subject of numerous studies, since it is a good model for the investigation of hydrogen bonding and proton transfer in enzymes and other systems containing aryl alcohols. In contrast to the data for phenol, relatively few data are available for para-substituted halophenols. As yet, the experimental gas-phase structures of *para*-chlorophenol (*p*-ClPh) and *para*-bromophenol (*p*-BrPh) are unknown. In a previous paper,¹ we reported a detailed study for phenol using HF, MP2, and DFT(BLYP) methods and showed that density functional is superior to the other methods (including MP2) in reproducing vibrational frequencies. In earlier experimental works,² the hydrogen-bonded complexes between the halophenol derivatives and purines or aliphatic amides have been investigated. Brzezinski et al.³ have studied the proton potential as a function of the *pK_a* of the para-substituted halophenols involved in the intermolecular hydrogen bonds. The experimental infrared spectra of *p*-ClPh and *p*-BrPh have been investigated by many workers.^{3–8} However, the reported band assignment is often contradictory. So far, the complete infrared intensities have not been published, and normal coordinate analyses have not been made for these molecules.

In this work, we have undertaken an extensive density functional study of the molecular structures, vibrational frequencies, and infrared intensities of *p*-ClPh, *p*-BrPh, and their OD counterparts. The theoretical studies were complemented by a detailed infrared spectroscopic investigation of these molecules. To obtain better insight into the nature of the normal modes,

we calculated the potential energy distributions. A clear-cut assignment of the vibrational spectra is reported which aims to clarify the contradictions encountered in earlier works. Interesting effects of the σ -electron-withdrawing substituents on the phenol ring geometry and on the characteristic phenolic frequencies and infrared intensities are presented.

Methods

Theoretical. To account for both the electronegativity and polarizability of the Cl and Br atoms, we have used the extended basis set of Pople and co-workers, 6-311++G(df,pd).^{9,10} This the valence triple- ζ basis set is augmented by polarization functions (sets of d and f polarization functions for heavy atoms and p and d functions for hydrogen) and supplemented by s, p, and d diffuse functions. This choice of basis set leads to 300 basis functions (460 primitives) for *p*-ClPh and 318 basis functions (501 primitives) for *p*-bromophenol, which is the largest such computation reported on these molecules to date. The geometries of the molecules were optimized with the MP2, HF, and DFT methods. Among the density functionals, the following were applied: three-parameter hybrid methods, B3LYP^{11,12} and B3PW91,¹³ and a one-parameter hybrid method, mPWIPW91, introduced recently by Adamo and Barone.¹⁴

Initially, the geometry optimizations were performed under the relaxation of all internal degrees of freedom, and the results revealed that both molecules are planar. To obtain the symmetry of normal modes, we reoptimized the structures of these molecules assuming the *C_s* point group symmetry. Thereafter, vibrational frequencies and infrared intensities were calculated with the DFT and HF methods. Normal coordinate analyses were performed, as described previously for six-membered cyclic molecules.¹⁵ The influence of CCl₄ solvent on the spectra was

* Corresponding author. E-mail: michalska@ichn.ch.pwr.wroc.pl.

[†] Technical University of Wrocław.

[‡] University of Leuven.

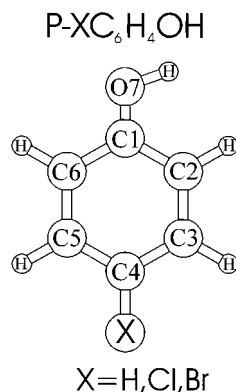


Figure 1. Atom numbering in the studied molecules.

TABLE 1. Bond Lengths (Å) and Bond Angles (deg) of *p*-Bromophenol and *p*-Chlorophenol (*p*- $\text{XC}_6\text{H}_4\text{OH}$, X = Br or Cl) Optimized with MP2 and B3LYP Methods Using the 6-311++G(df,pd) Basis Set^a

	MP2/6-311++G(df,pd)			B3LYP/6-311++G(df,pd)	
	X = H	X = Br	X = Cl	X = Br	X = Cl
C4-X	1.0840	1.8848	1.7282	1.9133	1.7579
C1-O7	1.3649	1.3629	1.3636	1.3651	1.3658
O7-H	0.9602	0.9603	0.9603	0.9622	0.9621
C1-C2	1.3959	1.3956	1.3954	1.3934	1.3930
C2-C3	1.3952	1.3948	1.3943	1.3914	1.3909
C3-C4	1.3937	1.3927	1.3917	1.3873	1.3873
C4-C5	1.3963	1.3957	1.3943	1.3906	1.3904
C5-C6	1.3923	1.3915	1.3912	1.3879	1.3875
C6-C1	1.3955	1.3957	1.3954	1.3937	1.3935
C2-H	1.0869	1.0867	1.0866	1.0846	1.0846
C3-H	1.0849	1.0839	1.0839	1.0813	1.0812
C5-H	1.0849	1.0839	1.0840	1.0814	1.0813
C6-H	1.0842	1.0843	1.0841	1.0819	1.0819
C1-C2-C3	119.80	120.28	120.24	120.20	120.23
C2-C3-C4	120.40	119.55	119.65	119.53	119.52
C3-C4-C5	119.39	120.47	120.36	120.63	120.63
C4-C5-C6	120.63	119.74	119.86	119.76	119.76
C5-C6-C1	119.64	120.16	120.11	120.05	120.07
C6-C1-C2	120.14	119.80	119.78	119.83	119.80
C5-C4-X	120.34	119.78	119.82	119.67	119.65
C6-C1-O7	117.21	117.28	117.28	117.40	117.41
C1-O7-H	108.11	108.35	108.30	110.04	110.04
C3-C2-H	120.23	119.56	119.63	119.58	119.59
C5-C6-H	121.45	120.83	120.86	120.76	120.78
C4-C3-H	120.24	120.31	120.03	120.48	120.26
C4-C5-H	120.05	120.13	119.86	120.28	120.04

^a The MP2-optimized geometry of phenol is included for comparison.

studied using the Onsager model.¹⁶ The changes in the B3LYP-calculated frequencies were less than 3 cm^{-1} (including the "sensitive" OH stretching modes), which indicated that the theoretical results obtained for the gas-phase molecules could be used for the interpretation of the experimental spectra recorded in inert solvents.

All calculations have been carried out with the Gaussian 98 package¹⁷ running on Cray J916 and CSGI Origin 2000 supercomputers.

Experimental. The FT-IR spectra of *p*-ClPhenol and *p*-BrPhenol and their OD counterparts were measured at 298 K in carbon tetrachloride ($3700\text{--}850\text{ cm}^{-1}$) and cyclohexane ($850\text{--}400\text{ cm}^{-1}$) solutions at a concentration of 0.05 mol dm^{-3} . The spectra were recorded on a Bruker 66 FT-IR spectrometer equipped with a KBr beam splitter, a Globar source, and a DTGS detector. The spectra were recorded at 2 cm^{-1} resolution using a KBr liquid cell. The integrated intensities were determined using the Bruker OPUS software, and overlapping bands were deconvoluted with the same software. Bands characterized

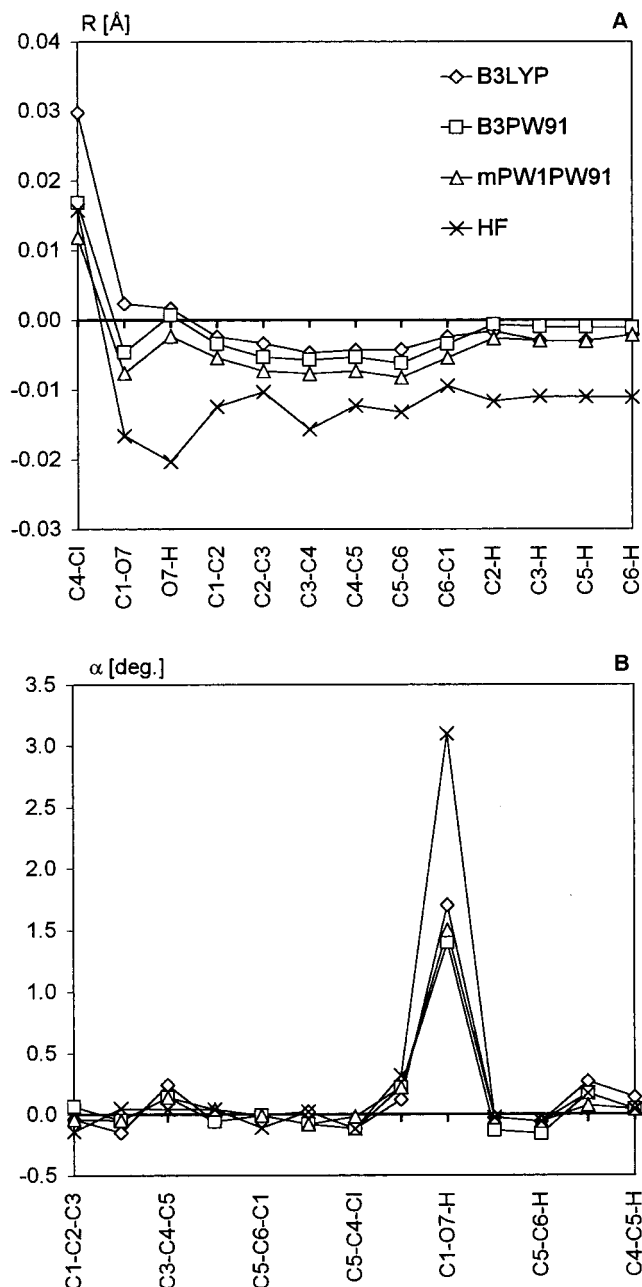


Figure 2. (A) Differences between the bond lengths of *p*-ClPh calculated with the B3LYP, mPW1PW, and HF methods and those computed at the MP2 level. (B) Differences between the corresponding bond angles calculated with these methods.

by a very weak IR intensity (νCH vibrations) were recorded in extended scale.

The phenols, purchased from Aldrich, were recrystallized from a petroleum-ether mixture. The solvents from Janssen Chimica were dried on molecular sieves. Phenol-ODs were prepared by several exchanges in methanol-OD (Cambridge Isotope Laboratories, 99%). About 90% deuteration was achieved. For reliable results, the infrared intensities of the $\nu(\text{OD})$ and $\delta(\text{OD})$ bands were multiplied by a factor of 1.1.

Results and Discussion

A. Structural Parameters. An accurate prediction of the geometrical parameters for *p*-ClPh and *p*-BrPh is of special interest because there is no experimental structure reported for these molecules in the gas-phase.

TABLE 2: Vibrational Frequencies (cm⁻¹), IR Intensities (km mol⁻¹), and Band Assignments for *p*-Chlorophenol (*p*-ClPh)

	sym	exp.			B3LYP/6-311++G(df, pd)		PED ^d [%]
		ν^a	<i>A</i>	<i>I</i> _{Rel} ^b	ω^c	<i>A</i>	
Q1	A''				123	0	τ_3 ring(54), γ CCl(25), τ_2 ring(19)
Q2	A'				256	2	δ CCl(76), δ CO(13), ν (C-C)(10)
Q3	A''	303 ^e			300	102	τ OH(95)
Q4	A''	331 ^f			320	10	γ CCl(42), τ_1 ring(28), γ CO(22)
Q5	A'	382 ^f			373	1	δ_2 ring(48), ν (C-Cl)(38)
Q6	A''				414	1	τ_2 ring(75), τ_3 ring(25)
Q7	A'	423	0.9	3	417	10	δ CO(65), δ_3 ring(15), δ CCl(13)
Q8	A''	501	4.0	11	503	21	γ CO(40), τ_3 ring(25), γ CCl(12)
Q9	A'	644	5.7	16	633	42	ν (C-Cl)(36), δ_2 ring(26), ν (C-O)(13)
Q10	A'	no			637	1	δ_3 ring(75)
Q11	A''	668	0.5	1	675	0	τ_1 ring(85), γ CO(15)
		768	1.1				
Q12	A''	788	13.6	37	793	19	γ C ₂ H(63), γ C ₃ H(26)
Q13	A'	no			822	2	ν (C-C)(45), ν (C-O)(22), δ_2 ring(16)
Q14	A''	823	11.3	31	822	47	γ C ₆ H(52), γ C ₃ H(34), γ CO(14)
Q15	A''	no			908	1	γ C ₃ H(61), γ C ₃ H(27), γ C ₅ H(12)
Q16	A''	no			949	0	γ C ₅ H(51), γ C ₆ H(40)
Q17	A'	1010	2.3	6	1007	9	δ_1 ring(56), ν (C-C)(30), δ CH(11)
Q18	A'	1096	19.7	54	1081	34	ν (C ₄ -C ₅)(24), ν (C ₃ -C ₄)(19), ν (C-Cl)(19)
Q19	A'	1112	0.3	1	1102	26	δ CH(53), ν (C-C)(38)
Q20	A'	1166 ^g	20.4	56	1171	8	δ CH(77), ν (C-C)(22)
Q21	A'	1176 ^g	35.6	97	1164 ^h	173	δ OH(55), ν (C ₁ -C ₆)(15), δ C ₆ H(11)
Q22	A'	1259	35.3	96	1260	108	ν (C-O)(51), ν (C-C)(23), δ CH(16)
Q23	A'				1293	2	δ CH(44), ν (C ₃ -C ₄)(21), ν (C ₄ -C ₅)(20)
Q24	A'	1320	4.8	13	1328	25	δ CH(43), ν (C-C)(35), δ OH(19)
		1341	0.6				
Q25	A'	1424	11.1	30	1430	24	ν (C-C)(45), δ CH(34), δ OH(10)
Q26	A'	1494	60.4	165	1497	152	δ CH(56), ν (C ₃ -C ₄)(13)
Q27	A'	1594	9.4	26	1597	17	ν (C ₁ -C ₂)(28), ν (C ₄ -C ₅)(20)
Q28	A'	1606	6.5	18	1611	18	ν (C ₁ -C ₆)(22), ν (C ₂ -C ₃)(17), ν (C ₅ -C ₆)(16), ν (C ₃ -C ₄)(12)
Q29	A'	3010	2.1	6	3096	13	ν (C ₂ -H)(97)
Q30	A'	3038	vw		3129	2	ν (C ₆ -H)(67), ν (C ₅ -H)(33)
Q31	A'	3064	vw		3140	2	ν (C ₃ -H)(94)
Q32	A'	3073	vw		3144	1	ν (C ₅ -H)(64), ν (C ₆ -H)(32)
Q33	A'	3609	55.9	151	3758	71	ν (O-H)(100)

^a From the IR spectra of cyclohexane and CCl₄ solutions. Abbreviations: no, not observed; vw, very weak. ^b *I*_{Rel}, integral absorbances of absorption bands normalized in such a way that the observed intensity sum of all bands is equal to the B3LYP-calculated intensity sum of the corresponding modes. ^c Frequencies scaled by 0.98. ^d Predominant contributions (those below 10% are summarized and given as a total). ^e Ref 8 (cyclohexane solution). ^f Ref 5 (solid). ^g Fermi resonance. ^h Reordered modes.

According to the results obtained with all the theoretical methods, both the *p*-BrPh and *p*-ClPh molecules are planar. Figure 1 shows the numbering of atoms of the title molecules. In Table 1 are listed the theoretical bond lengths and bond angles of *p*-BrPh and *p*-ClPh, optimized with the MP2 and B3LYP methods using the 6-311++G(df,pd) basis set (tables with the results obtained from the remaining theoretical methods are available as Supporting Information). The geometrical parameters of the parent phenol have also been calculated at the MP2/6-311++G(df, pd) level in this work, and they show very good agreement with the experimental results reported for phenol in refs 1 and 18. Thus, it is expected that the structures of *p*-chloro and *p*-bromo derivatives of phenol, optimized at the same level of theory, should be quite accurate.

As is seen in Table 1, the C-Br and C-Cl bond lengths in these molecules are 1.8848 and 1.7282 Å, respectively. The B3LYP functional yields C-Br and C-Cl distances longer than the MP2 values by about 0.03 Å. All the theoretical methods consistently indicate that the C-O bond in *p*-BrPh is slightly shorter than that in *p*-ClPh. Moreover, according to the MP2 results, this bond is shorter than that in the parent phenol. The MP2-calculated C-O bond lengths are as follows: 1.3629 Å for *p*-BrPh, 1.3636 Å for *p*-ClPh, and 1.3649 Å for phenol. It is quite striking, however, that the calculated phenolic OH bond length is almost unaffected by the ring substitution, as shown in Table 1. It should be emphasized that the OH bond distance

in the parent phenol computed by the MP2 method (0.960 Å) is in excellent agreement with the experimental value of 0.958 Å recently reported for phenol vapor.¹⁸

The MP2-calculated CC bond lengths and angles, although only slightly different in the studied molecules, show the sensitivity of electron density distribution toward para-substitution at the phenol ring. It is seen from Table 1 that the C-C bond lengths systematically decrease in the series phenol > *p*-BrPh > *p*-ClPh. The most pronounced changes are noted for the C₃-C₄ and C₄-C₅ bonds adjacent to the substituents. These changes are on the magnitude of 0.002 Å in *p*-ClPh and 0.001 Å in *p*-BrPh. Moreover, the MP2 results reveal small distortions of the CCC angles in the ring. The C₃C₄C₅ angle at the position of Cl/Br substituent is larger, whereas the two neighboring angles, C₂C₃C₄ and C₄C₅C₆, are smaller than those in phenol by about 1°. It is interesting that the MP2-predicted regular shortening of the C₃-C₄ and C₄-C₅ bonds follows the order of increasing electronegativity of the atoms: H < Br < Cl. Thus, substitution at the 4 position of the phenol ring by the σ -electron-withdrawing atom (Br or Cl) leads to a slight shortening of the adjacent CC bonds and to an opening of the corresponding CCC angle. These geometric changes have been thoroughly discussed for monosubstituted benzenes.^{19,20} According to the results obtained at the MP2 level, the C₂-C₃ and C₅-C₆ bonds are slightly shortened by about 0.001 Å in *p*-ClPh and by less than 0.001 Å in *p*-BrPh compared to those

TABLE 3: Vibrational Frequencies (cm⁻¹), IR Intensities (km mol⁻¹), and Band Assignments for *p*-Chlorophenol-OD (*p*-ClPh-OD)^a

	sym	exp.			B3LYP/6-311++G(df, pd)		PED [%]
		ν	<i>A</i>	<i>I</i> _{Rel}	ω	<i>A</i>	
Q1	A''				121	0	τ_3 ring(53), γ CCl(24), τ_2 ring(19)
Q2	A''	227			222	57	τ OD(98)
Q3	A'				253	2	δ CCL(72), δ CO(16), ν (C-C)(11)
Q4	A''				320	3	γ CCL(45), τ_1 ring(30), γ CO(22)
Q5	A'				370	2	δ_2 ring(47), ν (C-Cl)(37)
Q6	A'				401	9	δ CO(61), δ CCL(15), δ_3 ring(14)
Q7	A''	419	0.7	2	414	0	τ_2 ring(76), τ_3 ring(24)
Q8	A''	501	13.5	31	503	18	γ CO(40), τ_3 ring(26), γ CCL(12)
Q9	A'	641	21.2	49	629	36	ν (C-Cl)(35), δ_2 ring(23), ν (C-O)(13)
Q10	A'	no			636	3	δ_3 ring(74), ν (C-C)(12)
Q11	A''	697	0.3	1	675	0	τ_1 ring(83), γ C ₁ O(17)
Q12	A''	799	2.1	5	793	17	γ C ₂ H(63), γ C ₃ H(26)
Q13	A'	no			816	0	ν (C-C)(45), ν (C ₁ -O)(19), δ_2 ring(18)
Q14	A''	823	42.1	98	822	50	γ C ₆ H(52), γ C ₅ H(34), γ CO(14)
Q15	A''	no			908	1	γ C ₃ H(69), γ C ₂ H(31), γ C ₅ H(12)
		938	1.8				
Q16	A'	918	7.3	17	912	82	δ OD(81)
Q17	A''	no			949	0	γ C ₅ H(57), γ C ₆ H(44), γ C ₃ H(10)
Q18	A'	1010	4.1	10	1007	12	δ_1 ring(56), ν (C ₁ -C ₂)(13), ν (C ₁ -C ₆)(11)
Q19	A'	1093	20.7	48	1082	46	ν (C ₄ -C ₅)(24), ν (C ₃ -C ₄)(20), ν (C-Cl)(20)
Q20	A'	1112	0.2	1	1108	11	δ CH(62), ν (C-C)(33)
Q21	A'	1165	20.6	44	1171	15	δ CH(78), ν (C-C)(21)
		1176	18.9				
Q22	A'	1252	54.1	125	1253	152	ν (C ₁ -O)(52), ν (C-C)(22), δ_1 ring(10)
		1280	0.5				
Q23	A'	1298	1.5	3	1291	4	ν (C-C)(81), δ CH(18)
Q24	A'	1321	0.5	1	1306	8	δ CH(71), ν (C-C)(23)
Q25	A'	1412	1.1	2	1418	4	ν (C-C)(51), δ CH(37)
		1424	1.7				
Q26	A'	1492	69.1	160	1496	175	δ CH(57), ν (C-C)(41)
Q27	A'	1590	3.2	7	1591	5	ν (C ₁ -C ₂)(25), ν (C ₄ -C ₅)(20), ν (C ₁ -C ₆)(14)
Q28	A'	1601	11.9	28	1609	30	ν (C ₅ -C ₆)(21), ν (C ₂ -C ₃)(20), ν (C ₁ -C ₆)(15)
Q29	A'	2666	30.5	71	2735	46	ν (O-D)100
Q30	A'	3029	2.5	6	3096	14	ν (C ₂ -H)(97)
Q31	A'	3038	vw		3129	2	ν (C ₆ -H)(67), ν (C ₅ -H)(33)
Q32	A'	3059	vw		3140	2	ν (C ₃ -H)(94)
Q33	A'	3072	vw		3144	1	ν (C ₅ -H)(64), ν (C ₆ -H)(32)

^a Same abbreviations as those under Table 2.

in the parent phenol. These effects coupled with the shortening of the C-O bond may be due to electron density delocalization within the aromatic ring. It seems that the C-C distances are governed chiefly by the electronegativity of the substituents and, to a less extent, by resonance factors. A considerable contribution of the quinoid structure is not justified for the title molecules, which is in agreement with the gas-phase studies on the acidity of para-substituted derivatives of phenols and related systems.²¹ It is also interesting to note that the exocyclic CCH angles for hydrogen atoms in the ortho position to the chlorine or bromine atom show a small dependence on the substituent. All theoretical methods have revealed that the C₄C₃H and C₄C₅H angles in *p*-ClPh are smaller than those in *p*-BrPh by about 0.3°. This may be attributed to the fact that the Cl...H interaction is slightly stronger than the Br...H interaction.

The performance of different methods in predicting molecular structures of the title molecules is illustrated in Figure 2 for *p*-ClPh (very similar results have been obtained for *p*-BrPh). As follows from Figure 2A, the HF method yields C-O, O-H, C-C, and C-H atom distances that are too short compared to the results obtained with the MP2 and DFT methods. Furthermore, it is apparent from Figure 2B that the HF method overestimates the COH angle by about 3°. The bond lengths calculated with all the DFT methods are very similar to the corresponding MP2 results, except for the C-Cl bond length, which is slightly overestimated with density functionals (by 0.012–0.030 Å). The DFT-predicted values of the CCC, CCX,

and CCH bond angles agree with the MP2 results; however, the DFT-optimized COH angle is slightly larger (by 1.2–1.5°). It should be emphasized that the MP2-optimized COH angle for phenol, 108.11° (this work), is in excellent agreement with the value of 108.8 ± 0.4° determined for phenol vapor by microwave studies.¹⁸

B. Infrared Spectra. The infrared spectra of *p*-ClPh-OH and *p*-ClPh-OD (in CCl₄ solution), in the frequency range of 1650–800 cm⁻¹, are illustrated in Figure 2. The theoretical infrared spectra of *p*-ClPh, *p*-BrPh, and their OD-deuterated derivatives, calculated with different theoretical methods, were compared with the experimentally determined frequencies and infrared intensities of these molecules. The best overall agreement between the calculated and experimental spectra has been obtained at the B3LYP/6-311++G(df, pd) level; therefore, only these theoretical results are presented along with the experimental data in Tables 2–5. Vibrational assignments are made on the basis of the calculated potential energy distribution (PED).

OH Vibrations. In the title molecules, the frequencies of the OH stretching and torsional vibrations are the most sensitive to intermolecular interactions and can be used as a sensitive probe for studying hydrogen bonding or self-association. Moreover, Fateley and co-workers⁸ have shown that the OH torsional frequency is directly related to the π -electron distortions in aromatic systems. These authors investigated the OH torsional vibration in the para-substituted phenols and have concluded that π -electron-donating substituents lower the OH torsional

TABLE 4: Vibrational Frequencies (cm⁻¹), IR Intensities (km mol⁻¹), and Band Assignments for *p*-Bromophenol (*p*-BrPh)^a

	sym	exp.			B3LYP/6-311++G(df, pd)		PED [%]
		ν	<i>A</i>	<i>I</i> _{Rel}	ω	<i>A</i>	
Q1	A''				109	0	τ_3 ring(48), γ CBr(33), τ_2 ring(17)
Q2	A'				215	1	δ CBr(82)
Q3	A'				284	1	ν (C-Br)(58), δ_2 ring(31)
Q4	A''				302	31	τ OH(38), γ CBr(31), τ_1 ring(19)
Q5	A''				311	81	τ OH(62), γ CBr(15), γ CO(11)
Q6	A''				411	1	τ_2 ring(75), τ_3 ring(25)
Q7	A'	417	1.5	4	412	11	δ CO(70), δ_3 ring(14)
Q8	A''	500	4.8	12	497	19	γ CO(39), τ_3 ring(26), γ CBr(10)
Q9	A'	606	3.5	9	596	31	δ_2 ring(44), ν (C-Br)(25), ν (C-O)(13)
Q10	A'	649	0.0	0	635	0	δ_3 ring(77)
Q11	A''	668	2.4	6	650	0	τ_1 ring(83), γ CO(17)
Q12	A''	788	4.2	11	792	23	γ C ₂ H(67), γ C ₃ H(26)
Q13	A'	798	0.5	1	818	2	ν (C-C)(42), ν (C-O)(23), δ_2 ring(16)
Q14	A''	821	10.6	28	820	40	γ C ₆ H(55), γ C ₅ H(34), γ CO(13)
Q15	A''	no			904	1	γ C ₃ H(62), γ C ₂ H(27), γ C ₅ H(11)
Q16	A''	no			949	0	γ C ₅ H(52), γ C ₆ H(38), γ C ₃ H(10)
Q17	A'	1012	9.4	24	1003	15	δ_1 ring(58), ν (C-C)(29)
Q18	A'	1071	14.1	37	1062	20	ν (C ₄ -C ₅)(29), ν (C ₃ -C ₄)(24), ν (C-Br)(12)
Q19	A'	1093	8.7	22	1102	22	ν (C ₂ -C ₃)(17), ν (C ₅ -C ₆)(15), δ C ₅ H(15)
		1108	1.0				
Q20	A'	1167	33.8	87	1173	8	δ CH(76), ν (C-C)(22)
Q21	A'	1176	18.8	49	1164*	181	δ OH(54), ν (C ₁ -C ₆)(15), δ C ₆ H(12)
Q22	A'	1259	47.3	122	1260	126	ν (C-O)(51), ν (C-C)(23), δ CH(16)
Q23	A'				1293	3	ν (C-C)(58), δ CH(40)
Q24	A'	1320	8.9	23	1327	24	δ CH(49), ν (C-C)(33), δ OH(18)
Q25	A'	1423	19.9	51	1427	25	ν (C-C)(45), δ CH(34), δ OH(10)
Q26	A'	1489	62.5	162	1493	139	δ CH(56), ν (C-C)(43)
Q27	A'	1590	12.8	33	1594	24	ν (C ₁ -C ₂)(29), ν (C ₄ -C ₅)(19)
Q28	A'	1601	1.7	5	1607	19	ν (C ₁ -C ₆)(25), ν (C ₂ -C ₃)(16), ν (C ₃ -C ₄)(14), ν (C ₅ -C ₆)(14)
Q29	A'	3000	2.4	6	3096	13	ν (C ₂ -H)(97)
Q30	A'	3012	0.8	2	3128	2	ν (C ₆ -H)(62), ν (C ₅ -H)(38)
Q31	A'	3035	vw		3138	2	ν (C ₃ -H)(94)
Q32	A'	3060	vw		3142	1	ν (C ₅ -H)(60), ν (C ₆ -H)(37)
Q33	A'	3607	47.2	122	3756	73	ν (O-H)(100)

^a Same abbreviations as those under Table 2.

frequency. This has been confirmed by our calculations. For *p*-ClPh (Table 2), the B3LYP-predicted frequency of the OH torsional vibration (Q3), 300 cm⁻¹, is in nearly perfect agreement with the experimental values, 302 cm⁻¹ (vapor) and 303 cm⁻¹ (cyclohexane solution).⁸ In the unsubstituted phenol, the OH torsional vibration has been assigned at higher frequencies, 309.2 cm⁻¹ (vapor) and 310 cm⁻¹ (cyclohexane solution).⁸ The analogous effect has been noticed for the deuterated derivatives. As shown for *p*-ClPh-OD (Table 3), the calculated frequency of the OD torsion (Q2), 222 cm⁻¹, is in very good agreement with the experimental value of 227 cm⁻¹. In the deuterated phenol, the OD torsion has also been observed at a higher frequency, 247 cm⁻¹.⁸

According to the PED calculated for *p*-BrPh (Table 4), the OH torsional vibration is coupled with the CBr out-of-plane vibration, γ (CBr). Thus, the effect of the para-substitution on the OH torsional frequency is less evident. However, in *p*-BrPh-OD, the OD torsion is a "pure" vibration (mode Q3 in Table 5). The B3LYP-calculated frequency of this mode, 226 cm⁻¹, is in excellent agreement with the experimental frequency, 228 cm⁻¹.⁸ The results obtained in our studies clearly demonstrate that both the OH and OD torsional vibrations are sensitive to the para-substitution of the phenol ring.

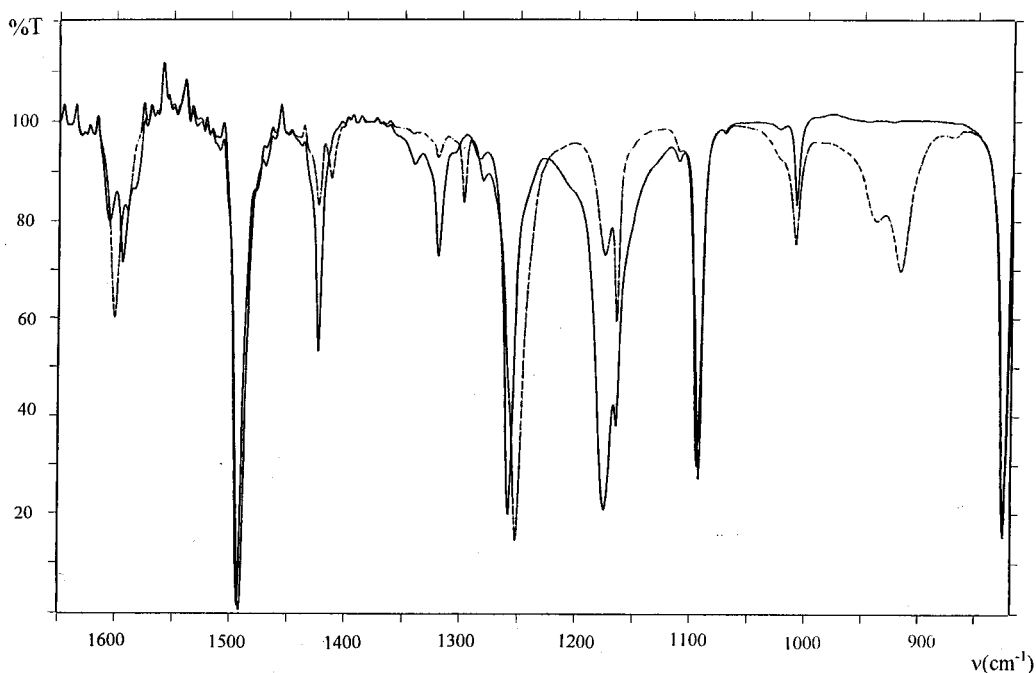
As shown in Tables 2 and 4, the OH stretching vibration (Q33) is observed at 3609 and 3607 cm⁻¹ in *p*-Cl and *p*-Br derivatives of phenol, respectively (in CCl₄). For phenol (in CCl₄) the corresponding ν (O-H) occurs at 3611 cm⁻¹ (our data). It should be noted that in the vapor phase of *p*-ClPh and

*p*BrPh, the OH stretching vibrations are observed at higher frequencies, 3657²² and 3655 cm⁻¹ [NIST Chemistry Web-Book], which may indicate some intermolecular interaction in CCl₄ solution. The calculated harmonic OH stretching frequencies are overestimated, since these vibrations are known to be strongly anharmonic. Nevertheless, all the DFT methods consistently indicate that the OH stretching vibration in *p*-ClPh is very slightly higher by 2 cm⁻¹ when compared to the *p*-BrPh derivative, and this is in accordance with the experimental data.

In our previous DFT calculations of unsubstituted phenol,¹ it has been shown that the OH in-plane bending vibration, δ -(OH), contributes mainly to two modes, observed at 1176 and 1343 cm⁻¹, in the gas-phase spectrum. Very similar results have been obtained in this work for the *p*-Cl and *p*-Br derivatives of phenol. As shown for *p*-ClPh (Table 2), the mode Q21 has predominant contribution (55%) from the OH in-plane bending vibration, and it has been assigned to the very strong band at 1176 cm⁻¹. This assignment is in very good agreement with the large blue shift (50 cm⁻¹) of this band observed in hydrogen-bonded complexes involving *p*-ClPh and N,N-dimethylacetamide.^{2a} The normal mode Q24 also involves significant contribution from the δ (OH) vibration (19%) and is attributed to the absorption at 1320 cm⁻¹. The B3LYP-predicted frequency, 1328 cm⁻¹ for mode Q24, is in very good agreement with experimental. The OH in-plane bending vibration contributes also (about 10%) to the mode Q25, assigned at 1424 cm⁻¹ (Table 2). As is seen in Figure 3, all these bands are sensitive to the deuteration of the phenolic OH group, which supports

TABLE 5: Vibrational Frequencies (cm^{-1}), IR Intensities (km mol^{-1}), and Band Assignments for *p*-Bromophenol-OD (*p*-BrPh-OD)^a

	sym	exp.			B3LYP/6-311++G(df, pd)		PED [%]
		ν	A	I_{Rel}	ω	A	
Q1	A''				107	0	$\tau_3\text{ring}(48)$, $\gamma\text{CBr}(32)$, $\tau_2\text{ring}(17)$
Q2	A'				212	1	$\delta\text{CBr}(80)$, $\delta\text{CO}(10)$
Q3	A''	228			226	55	$\tau\text{OD}(98)$
Q4	A'				282	1	$\nu(\text{C}-\text{Br})(57)$, $\delta_2\text{ring}(31)$
Q5	A''				306	5	$\gamma\text{CBr}(44)$, $\tau_1\text{ring}(26)$, $\gamma\text{CO}(21)$
Q6	A'	419	1.3	4	394	11	$\delta\text{CO}(67)$, $\delta_3\text{ring}(13)$, $\delta\text{CBr}(10)$
Q7	A''	no			410	0	$\tau_2\text{ring}(75)$, $\tau_3\text{ring}(25)$
Q8	A''	500	16.9	45	497	16	$\gamma\text{CO}(39)$, $\tau_3\text{ring}(26)$, $\gamma\text{CBr}(10)$
Q9	A'	601	14.7	39	592	27	$\delta_2\text{ring}(42)$, $\nu(\text{C}-\text{Br})(25)$, $\nu(\text{C}-\text{O})(13)$
Q10	A'	no			634	1	$\delta_3\text{ring}(78)$
Q11	A''	no			650	0	$\tau_1\text{ring}(83)$, $\gamma\text{CO}(17)$
Q12	A''	799	3.6	9	792	22	$\gamma\text{C}_2\text{H}(67)$, $\gamma\text{C}_3\text{H}(26)$
Q13	A'	no			811	0	$\nu(\text{C}-\text{C})(39)$, $\nu(\text{C}-\text{O})(20)$, $\delta_2\text{ring}(17)$
Q14	A''	821	23.3	62	819	44	$\gamma\text{C}_6\text{H}(55)$, $\gamma\text{C}_5\text{H}(34)$, $\gamma\text{CO}(13)$
Q15	A''	no			904	1	$\gamma\text{C}_3\text{H}(62)$, $\gamma\text{C}_2\text{H}(27)$, $\gamma\text{C}_5\text{H}(11)$
Q16	A'	918	7.0	18	912	83	$\delta\text{OD}(81)$
Q17	A''	no			949	0	$\gamma\text{C}_5\text{H}(52)$, $\gamma\text{C}_6\text{H}(38)$, $\gamma\text{C}_3\text{H}(10)$
Q18	A'	1010	6.2	16	1003	20	$\delta_1\text{ring}(62)$, $\nu(\text{C}_1-\text{C}_2)(13)$, $\nu(\text{C}_1\text{C}_6)(12)$
Q19	A'	1071	9.9	26	1062	26	$\nu(\text{C}_4-\text{C}_3)(29)$, $\nu(\text{C}_3-\text{C}_4)(25)$, $\nu(\text{C}-\text{Br})(12)$
		1097	1.7				
Q20	A'	1108	0.3	1	1108	11	$\delta\text{CH}(61)$, $\nu(\text{C}-\text{C})(34)$
Q21	A'	1167	3.9	10	1173	17	$\delta\text{CH}(77)$, $\nu(\text{C}-\text{C})(22)$
Q22	A'	1253	61.4	163	1253	172	$\nu(\text{C}-\text{O})(52)$, $\nu(\text{C}-\text{C})(22)$
		1277	0.3				
Q23	A'	1299	2.0	5	1290	5	$\nu(\text{C}-\text{C})(87)$, $\delta\text{CH}(10)$
Q24	A'	1320	0.8	2	1306	8	$\delta\text{CH}(77)$, $\nu(\text{C}-\text{C})(17)$
Q25	A'	1413	0.3	1	1413	4	$\nu(\text{C}-\text{C})(50)$, $\delta\text{CH}(38)$
Q26	A'	1487	64.5	171	1492	160	$\delta\text{CH}(59)$, $\nu(\text{C}-\text{C})(36)$
Q27	A'	1588	7.7	20	1588	8	$\nu(\text{C}_1-\text{C}_2)(27)$, $\nu(\text{C}_4-\text{C}_5)(20)$, $\nu(\text{C}_1-\text{C}_6)(13)$
Q28	A'	1595	10.0	26	1604	35	$\nu(\text{C}_5-\text{C}_6)(20)$, $\nu(\text{C}_2-\text{C}_3)(20)$, $\nu(\text{C}_1-\text{C}_6)(17)$
Q29	A'	2665	39.5	104	2734	47	$\nu(\text{O}-\text{D})(100)$
Q30	A'	3012	2.5	7	3096	14	$\nu(\text{C}_2-\text{H})(97)$
Q31	A'	3035	vw		3128	2	$\nu(\text{C}_6-\text{H})(62)$, $\nu(\text{C}_5-\text{H})(38)$
Q32	A'	3060	0.7	2	3138	2	$\nu(\text{C}_3-\text{H})(94)$
Q33	A'	3069	vw		3142	1	$\nu(\text{C}_5-\text{H})(60)$, $\nu(\text{C}_6-\text{H})(37)$

^a Same abbreviations as those under Table 2.**Figure 3.** IR spectra of *p*-chlorophenol-OH (---) and *p*-chlorophenol-OD (....) in the range of 1650–800 cm^{-1} . The solvent is carbon tetrachloride, $c = 0.05 \text{ mol}^{-3}$, and path length = 0.04 cm.

our assignment. For *p*-BrPh (Table 4) the corresponding bands are observed at almost identical frequencies, 1176 (Q21), 1320

(Q24), and 1423 cm^{-1} (Q25). We have reported previously for phenol that the absorption pattern around 1170 cm^{-1} is

complicated by some anharmonic resonances.¹ In this study, a very similar effect has been noted for *p*-ClPh and *p*-BrPh. The predicted infrared intensity is very low for Q20 and very high for Q21, as shown in Tables 2 and 4. However, in the experimental infrared spectra, the two corresponding bands are quite strong. This is probably caused by the "intensity borrowing" mechanism in multiple resonance effects. In the spectra of the deuterated derivatives, *p*-ClPhOD and *p*-BrPhOD (Tables 3 and 5), the new absorption band at 918 cm⁻¹ is assigned to the normal mode Q16 (*A'*), which corresponds to the OD in-plane bending vibration. As is seen in the spectrum of *p*-ClPhOD (Figure 3), there is also another band, at 938 cm⁻¹, which probably results from Fermi resonance between the fundamental mode Q16 and a combination tone of the *A'* symmetry (e.g., 228 + 799 = 924 cm⁻¹; *A''* × *A''* = *A'*).

C–X (Halogen) Vibrations. From the calculated potential energy distributions, it is possible to assign unequivocally all the normal modes involving the C–X (X = Cl or Br) vibrations. In the earlier experimental studies of the para-substituted phenols, the assignment of these vibrations was very uncertain.^{4–8} As follows from Table 2, the C–Cl stretching vibration is strongly coupled with ring vibrations, and it contributes mainly to three normal modes: Q5, Q9, and Q18. The calculated frequency of Q5 is about 380 cm⁻¹, which is in excellent agreement with the frequency of 382 cm⁻¹ reported for *p*-ClPh (solid).⁵ In our infrared spectrum, the medium-intensity band at 644 cm⁻¹ has been assigned to the mode Q9. As shown in Table 2, this mode involves a predominant contribution (36%) from the C–Cl stretching vibration. The strong band at 1096 cm⁻¹ (Q18 mode) arises from coupled vibration, which also involves the C–Cl stretching (19%). It should be mentioned that the corresponding mode in the unsubstituted phenol, (designated as 18a), is observed as a weak band, at 1026 cm⁻¹, in the infrared spectrum of phenol vapor.¹ Calculations performed for *p*-BrPh (Table 4) reveal that the mode Q3 has a predominant contribution from the C–Br stretching vibration. The predicted infrared intensity is very low; therefore, it may not be observed in the experimental spectrum. According to the PED, the Q9 mode also involves a contribution of the C–Br stretching vibration (25%), coupled with the in-plane deformation of the ring (44%). This mode has been assigned to the medium-intensity band, at 606 cm⁻¹, in the infrared spectrum of *p*-BrPh. The strong band at 1071 cm⁻¹ (mode Q18) also involves some contribution from the C–Br stretching vibration.

Thus, the two bands characteristic for *p*-ClPh are located at 644 and 1096 cm⁻¹, and the corresponding bands for *p*-BrPh are observed at 606 and 1071 cm⁻¹. The remaining substituent-sensitive modes arise from the CX in-plane (δ (CX)) and CX out-of-plane (γ (CX)) vibrations, and their assignments are shown in Tables 2–5.

CO Vibrations. In the gas spectrum of bare phenol, the C–O stretching vibration has been observed at 1261 cm⁻¹.²¹ In the infrared spectra of the *p*-Cl and *p*-Br derivatives, the corresponding vibration (Q22) is assigned to the very strong band at 1259 cm⁻¹ (Figure 3). This band is slightly shifted (to 1252 cm⁻¹) upon deuteration, which confirms our assignment. The B3LYP-calculated frequency for the Q22 mode, 1260 cm⁻¹, is in perfect agreement with the experimental value. The C–O stretching vibration also contributes to the mode Q13; however, due to a strong coupling with the ring deformations, the predicted infrared intensity for this mode is very low. Indeed, this band is not observed for *p*-ClPh, and it is extremely weak for *p*-BrPh. On the other hand, the corresponding vibration in phenol has a very large infrared intensity.¹

According to the PED, the CO in-plane bending (Q7) contributes mainly to the bands observed at 423 and 417 cm⁻¹ (for *p*-ClPh and *p*-BrPh, respectively).

Phenyl Ring Vibrations. The "ring breathing" vibration in phenol has been assigned to a weak band at 999 cm⁻¹ (the corresponding Raman line is very strong).²² In the infrared spectra of *p*-ClPh and *p*-BrPh, the "ring breathing" vibration (Q17) is also observed as a weak band at slightly higher frequencies, 1010 and 1012 cm⁻¹, respectively. Thus, a previous assignment of this mode to the band at 825–857 cm⁻¹ for a series of *p*-substituted phenols⁵ seems to be incorrect. In the infrared spectra of the title molecules, the most intense band is observed at 1494 cm⁻¹ (for *p*-ClPh) and 1489 cm⁻¹ (for *p*-BrPh), and it corresponds to the coupled vibration Q26, involving the δ (CH) (56%) and ν (CC) (42%). The other characteristic feature of the infrared spectra of *p*-ClPh and *p*-BrPh is the extremely low intensity of the "ring puckering mode" (Q11). In the infrared spectrum of phenol, the "ring puckering" vibration has been assigned to the strong band at 686 cm⁻¹.¹ In this work, all theoretical methods clearly indicate that mode Q11 has almost zero infrared intensity for both *p*-ClPh and *p*-BrPh. This is probably caused by the fact that the out-of-plane motion of the halogen atom (Cl or Br) in the para-position to the CO group nearly cancels the change of the dipole moment during the "ring-puckering" vibration.

The CH stretching vibrations of the title molecules are observed as weak bands in infrared, in the range of frequencies from 3000 to 3100 cm⁻¹. As revealed by calculations, the C–H bonds, being ortho to the chlorine or bromine substituent, are slightly shorter than the others, and this is reflected in the calculated frequencies of the C–H stretching vibrations. According to the PED, the C₅–H and C₆–H stretching vibrations are coupled as the in-phase (mode Q30) and out-of-phase (Q32) vibrations. These modes have been assigned to the bands at 3038 and 3073 cm⁻¹, respectively, for *p*-ClPh. It is interesting that of all the C–H stretching vibrations, the predicted infrared intensity is the largest for ν (C₂–H), mode Q29. It should be noted that the C₂–H bond is in close vicinity to the C₁OH group. Thus, a distinct infrared band at 3010 cm⁻¹ (for *p*-ClPh) has been assigned to the mode Q29.

As revealed by the PED, the two normal modes corresponding to the CH out-of-plane bending vibrations, Q12 and Q14, give rise to two medium-intensity bands at 788 and 823 cm⁻¹ for *p*-ClPh and at 799 and 823 cm⁻¹ for *p*-BrPh. The corresponding vibrations of the unsubstituted phenol appear at 751 and 881 cm⁻¹, respectively.¹ The assignments of the remaining fundamental transitions are given in Tables 2–5.

Acknowledgment. W. Z. and D. M. thank the Poznań Supercomputer and Networking Center as well as Wrocław Supercomputer and Networking Center for a generous computer time grant. T.Z.H. thanks the Fund of Scientific Research-Vlaanderen-Belgium for financial support. The authors are also indebted to Dr. N. Leroux for experimental assistance.

Supporting Information Available: Tables containing the optimized geometries and vibrational spectra calculated with the other theoretical methods (B3PW91, mPW1PW91, and HF using the 6-311++G(df, pd) basis set) are available from the authors upon request. This material is available free of charge via the Internet at <http://pubs.acs.org>.

References and Notes

- (1) Michalska, D.; Bieńko, D. C.; Abkowitz-Bieńko, A. J.; Latajka, Z. *J. Phys. Chem.* **1996**, *100*, 17786.

- (2) (a) Dorval, C.; Zeegers-Huyskens, Th. *Spectrochim. Acta* **1973**, *29A*, 1805. (b) Toppet, S.; De Taeye, J.; Zeegers-Huyskens, Th. *J. Phys. Chem.* **1988**, *92*, 6819. (c) Goethals, M.; Czarnik-Matusewicz, B.; Zeegers-Huyskens, Th. *J. Heterocycl. Chem.* **1999**, *36*, 49. (d) Leroux, N.; Samyn, C.; Zeegers-Huyskens, Th. *J. Mol. Struct.* **1998**, *448*, 209. (e) Rospenk, M.; Leroux, N.; Zeegers-Huyskens, Th. *J. Mol. Spectrosc.* **1997**, *183*, 245.
- (3) Brzezinski, B.; Brycki, B.; Zundel, G.; Keil, T. *J. Phys. Chem.* **1991**, *95*, 8598.
- (4) Cabana, A.; Patenaude, J. L.; Sandorfy, C.; Bavin, P. M. G. *J. Phys. Chem.* **1960**, *64*, 1941.
- (5) Jakobsen, R. J.; Brewer, E. J. *Appl. Spectrosc.* **1965**, *16*, 32.
- (6) (a) Hall, A.; Wood, J. L. *Spectrochim. Acta* **1967**, *23A*, 2657. (b) Hall, A.; Wood, J. L. *Spectrochim. Acta* **1972**, *28A*, 2331.
- (7) Green, J. H. S.; Harrison, D. J.; Kynaston, W. *Spectrochim. Acta* **1971**, *27A*, 2199.
- (8) Fateley, W. G.; Carlson, G. L.; Bentley, F. F. *J. Phys. Chem.* **1975**, *79*, 199.
- (9) Krishnan, R.; Binkley, J. S.; Seeger, R.; Pople, J. A. *J. Chem. Phys.* **1980**, *72*, 650.
- (10) Frisch, M. J.; Pople, J. A.; Binkley, J. S. *J. Chem. Phys.* **1984**, *80*, 3265.
- (11) Lee, C.; Yang, W.; Parr, R. G. *Phys. Rev. B* **1988**, *37*, 785.
- (12) (a) Becke, A. D. *J. Chem. Phys.* **1993**, *98*, 5648. (b) Becke, A. D. *J. Chem. Phys.* **1996**, *104*, 1040.
- (13) (a) Burke, K.; Perdew, J. P.; Wang, Y. In *Electronic Density Functional Theory: Recent Progress and New Directions*; Dobson, J. F., Vignale, G., Das, M. P., Eds.; Plenum: New York, 1998. (b) Perdew, J. P.; Burke, K.; Wang, Y. *Phys. Rev. B* **1996**, *54*, 16533. (c) Perdew, J. P.; Wang, Y. *Phys. Rev. B* **1992**, *45*, 13244.
- (14) Adamo, C.; Barone, V. *J. Chem. Phys.* **1998**, *108*, 664.
- (15) (a) Bieńko, D. C.; Michalska, D.; Roszak, S.; Wojciechowski, W.; Nowak, M. J.; Lapinski, L. *J. Phys. Chem. A* **1997**, *101*, 7834. (b) Abkowicz-Bieńko, A. J.; Latajka, Z.; Bieńko, D. C.; Michalska, D. *Chem. Phys.* **1999**, *250*, 123.
- (16) Wong, M. W.; Frisch, M. J.; Wiberg, J. *Am. Chem. Soc.* **1991**, *113*, 4776.
- (17) Frisch, M. J.; Trucks, G. W.; Schlegel, H. B.; Scuseria, G. E.; Robb, M. A.; Cheeseman, J. R.; Zakrzewski, V. G.; Montgomery, J. A.; Stratmann, R. E.; Burant, J. C.; Dapprich, S.; Millam, J. M.; Daniels, A. D.; Kudin, K. N.; Strain, M. C.; Farkas, O.; Tomasi, J.; Barone, V.; Cossi, M.; Cammi, R.; Mennucci, B.; Pomelli, C.; Adamo, C.; Clifford, S.; Ochterski, J.; Petersson, G. A.; Ayala, P. A.; Cui, Q.; Morokuma, K.; Malick, K. D.; Rabuck, A. D.; Raghavachari, K.; Foresman, J. B.; Cioslowski, J.; Ortiz, J. V.; Stefanov, B. B.; Liu, G.; Liashenko, A.; Piskorz, P.; Komaromi, I.; Gomperts, R.; Martin, R. L.; Fox, D. J.; Keith, T.; Al-Laham, M. A.; Peng, C. Y.; Nanayakkara, A.; Gonzales, C.; Challacombe, M.; Gill, P. M. W.; Johson, B. G.; Chen, W.; Wong, M.; Anders, J. L.; Head-Gordon, M.; Replogle, E. S.; Pople, J. A. *Gaussian 98*, Revision A1; Gaussian, Inc.: Pittsburgh, PA, 1998.
- (18) Portalone, G.; Schultz, G.; Domenicano, A.; Hargittai, I. *Chem. Phys. Lett.* **1992**, *197*, 482.
- (19) Topsom, R. D. In *Progress in Physical Organic Chemistry*; Taft, R. W., Ed.; John Wiley: New York, 1987; Vol. 16, p 85.
- (20) Krygowski, T. M. In *Progress in Physical Organic Chemistry*; Taft, R. W., Ed.; John Wiley: New York, 1990; Vol. 17, p 239.
- (21) Taft, R. W.; Topsom, R. D. In *Progress in Physical Organic Chemistry*; Taft, R. W., Ed.; John Wiley: New York, 1987; Vol. 16, p 1 and references herein.
- (22) Hartland, G. V.; Henson, B. F.; Venturo, V. A.; Felker, P. M. *J. Phys. Chem.* **1992**, *96*, 1164.